

Electronic Supplementary Information

Defective Graphene Anchored Iron-Cobalt Nanoparticles for Efficient Electrocatalytic Oxygen Reduction

Xuecheng Yan¹, Yi Jia¹, Longzhou Zhang¹, Mun Teng Soo², Xiangdong Yao^{1*}

¹ School of Natural Sciences and Queensland Micro- and Nanotechnology Centre, Griffith University, Nathan Campus, QLD 4111, Australia

² Materials Engineering, The University of Queensland, St. Lucia, QLD 4072, Australia

* Corresponding author. E-mail: x.yao@griffith.edu.au

Experimental Section

(1) Catalysts Preparation

The defective graphene (DG) was prepared *via* a simple nitrogen doping and removal method, as described elsewhere.¹ The FeCo nanoparticles were introduced into the DG by an impregnation method, followed by a calcination process in a tubular furnace under nitrogen conditions. Specifically, metal salt precursors iron(III) nitrate nonahydrate ($\text{Fe}(\text{NO}_3)_3 \cdot 9\text{H}_2\text{O}$) and cobalt(II) acetate tetrahydrate ($(\text{CH}_3\text{COO})_2\text{Co} \cdot 4\text{H}_2\text{O}$) were dissolved into a certain volume of ethanol, following by adding the DG powder. The mixture was then sonicated for 10 min. Afterwards, the solvent was evaporated under constant stirring conditions at room temperature in the fume cupboard. The final sample was obtained *via* calcining the dried precursor at 750 °C for 2 h under nitrogen conditions, which was denoted as DG@FeCo. Similarly, the single Fe or Co loaded DG samples and the FeCo decorated pristine graphene (G) were prepared by the same method, the resultant samples were denoted as DG@Fe, DG@Co and G@FeCo, respectively. For the preparation of pure FeCo alloy, FeCl_3 and CoCl_2 with the molar ratio of 1:1 were dissolved into the mixed solvent of ethylene glycol, distilled water and ethanol with the volume ratio of 2:1:1, following by the addition of NaAc and CTAB. The mixture was transferred into a 100 mL autoclave line after stirring for 1 h. Afterwards, the autoclave was placed into an oven and reacting at 200 °C for 24 h. The sample was collected by washing with ethanol and distilled water multiple times. The dried sample was reduced in a tubular furnace at 400 °C for 1 h under a hydrogen atmosphere, the resulting sample is denoted as FeCo.

(2) Characterizations

The morphology, metal particle size and energy-dispersive X-ray spectroscopy (EDS) elemental-mapping of the prepared samples were measured using transmission electron microscopy (TEM, Philips Tecnai F20). The crystalline structures of the synthesized catalysts were identified by XRD in a Bruker Advance X-ray diffractometer using $\text{Cu K}\alpha$ X-ray source radiation ($\lambda = 1.5405 \text{ \AA}$). The chemical composition and the surface state of the prepared samples were obtained by a Kratos

Axis ULTRA X-ray photoelectron spectrometer incorporating a 165 mm hemispherical electron energy analyzer, and the energy scale was calibrated to the C 1s peak maximum at 284.5 eV.

(3) Electrochemical Measurements

The typical three-electrode system was used to assess the ORR performance of the prepared catalysts. Specifically, glassy carbon (GC) is the working electrode, a Pt wire is the counter electrode and the Ag/AgCl (in saturated KCl solution) is the reference electrode. All potentials were referred to the reversible hydrogen electrode by adding a value of $(0.197 + 0.059 \cdot \text{pH})$ V and all the tests were performed without iR compensation. Cyclic voltammetry (CV), linear sweep voltammetry (LSV) and rotating ring-disk electrode (RRDE) measurements were conducted on the CHI 760E workstation (CH Instruments, Inc.) with a RRDE-3A rotator (ALS Co., Ltd).

Sample Preparation: 2 mg of the catalyst was dispersed into 1 mL mixed solution of distilled water (680 μL), ethanol (300 μL) and Nafion® 117 Solution (5%, 20 μL). The mixture was then sonicated for at least 60 min. Afterwards, 10 μL of the ink was dropped onto the polished glassy carbon electrode (4 mm in diameter, catalyst loading: 0.16 $\text{mg} \cdot \text{cm}^{-2}$). The loaded electrode was placed in a 60 °C oven allow it to dry under an atmospheric environment.

Prior to the CV test, the electrolyte (0.1 mol/L KOH solution) was bubbled with oxygen for at least 30 min to allow it saturated with oxygen, and a constant oxygen flow was maintained during the measurement. The data was recorded at a scan rate of 100 mV/s when the system became steady. For the LSV measurement, the rotating speed of the working electrode was increased from 400 to 2500 rpm at a scan rate of 10 mV/s in an O₂-saturated 0.1 M KOH solution.

Koutecky-Levich (K-L) Plots. The RDE was scanned at a rate of 10 mV/s with the rotation speed from 400 to 2500 rpm. Koutecky-Levich (K-L) plots (J^{-1} vs $\omega^{-1/2}$) were analyzed at different potentials.

Koutecky-Levich equation:^{2,3}

$$\frac{1}{J} = \frac{1}{J_L} + \frac{1}{J_K} = \frac{1}{B\omega^{1/2}} + \frac{1}{J_K}$$

$$B = 0.2nFC_0D_0^{2/3}\nu^{-1/6}; J_K = nFkC_0$$

where J is the measured current density, J_k and J_L are the kinetic and limiting current densities, respectively, ω is the angular velocity, n is transferred electron number, F (96485 C/mol) is the Faraday constant, D_0 is the diffusion coefficient of oxygen in 0.1 M KOH (1.9×10^{-5} cm²/s), C_0 is the bulk concentration of oxygen (1.2×10^{-6} mol/cm³), ν is the kinetic viscosity of the electrolyte (0.01 cm²/s) and k is the electron-transfer rate constant. The constant 0.2 is used when the rotation speed is expressed in rpm.

RRDE Measurement. The rotating speed of the working electrode was fixed at 1600 rpm with a scan rate of 10 mV/s in an O₂-saturated 0.1 M KOH solution for the RRDE test. The electron transfer number (n) and the percentage of HO₂⁻ and were calculated *via* the following equations.^{4,5}

$$n = 4I_d / (I_d + I_r / N) \quad (\text{S1})$$

$$\% \text{HO}_2^- = 200(I_r / N) / (I_d + I_r / N) \quad (\text{S2})$$

Where I_d stands for the disk current, I_r represents the ring current, and N is the current collection efficiency of the Pt ring, which was identified to be 0.43 in 2 mmol/L K₃Fe[CN]₆ and 0.1 mol/L KCl solution.

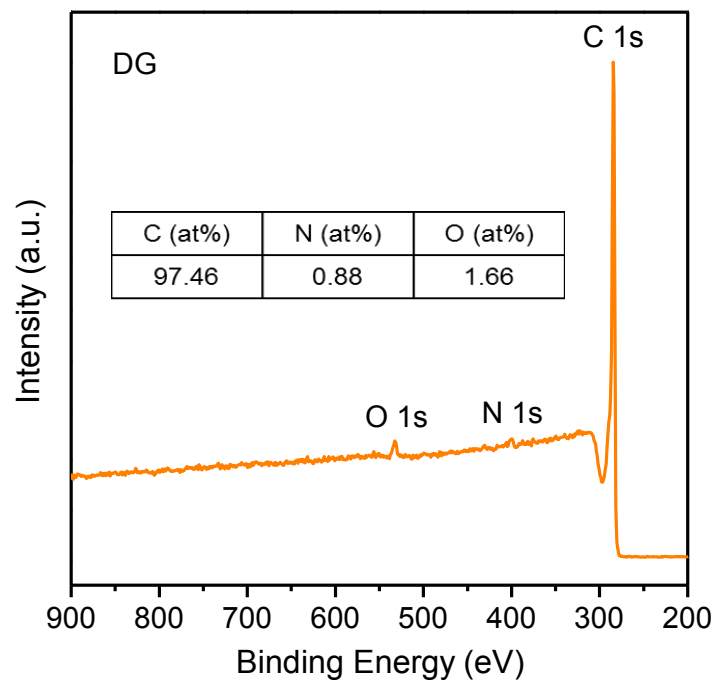


Fig. S1 XPS survey spectrum of the defective graphene (DG).

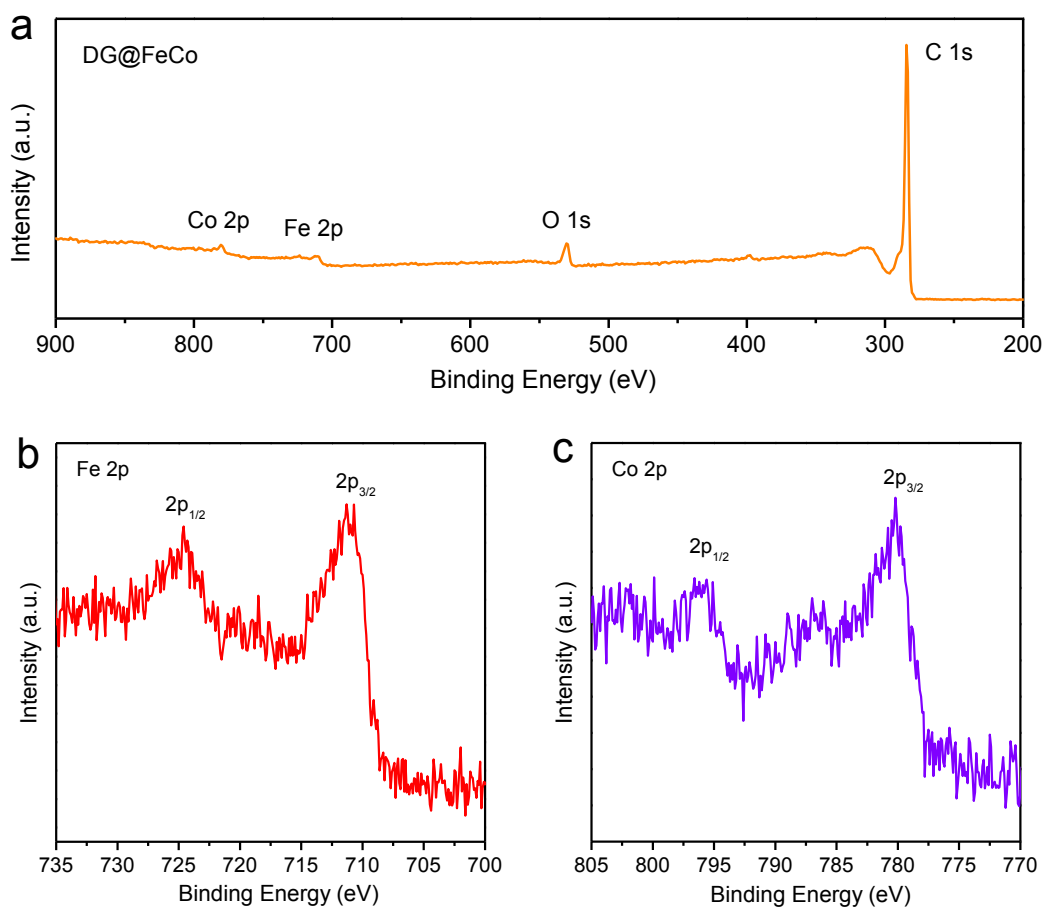


Fig. S2 (a) XPS survey spectrum of the prepared sample DG@FeCo; (b) High resolution Fe 2p XPS spectrum of DG@FeCo; (c) High resolution Co 2p XPS spectrum of DG@FeCo.

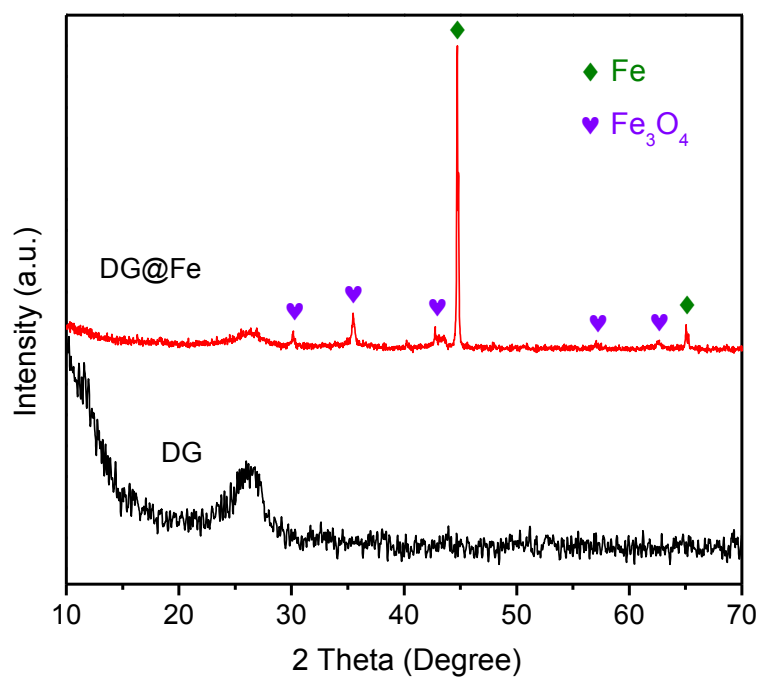


Fig. S3 XRD patterns of the DG and the synthesized sample DG@Fe.

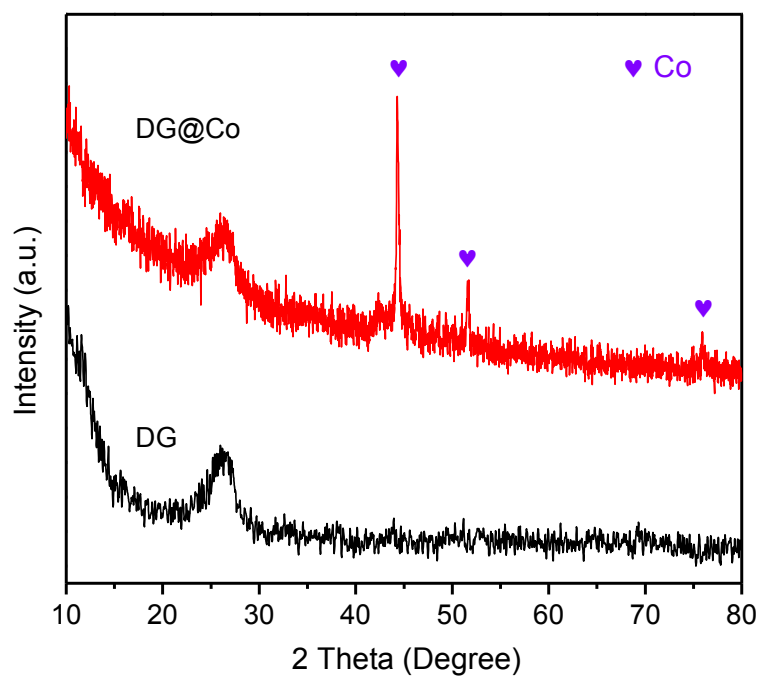


Fig. S4 XRD patterns of the DG and the synthesized sample DG@Co.

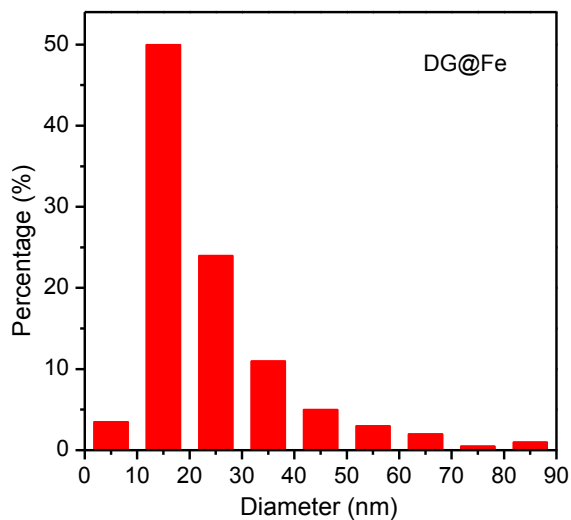
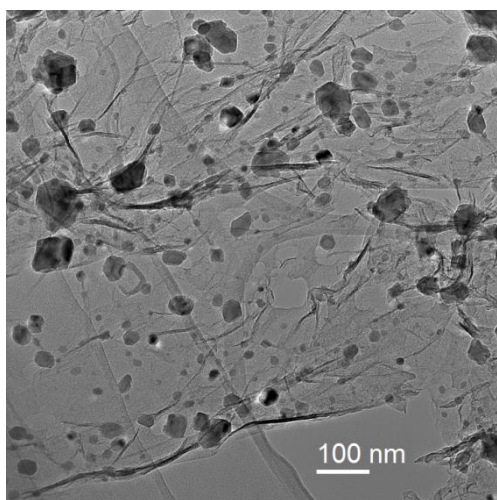


Fig. S5 TEM images of the prepared sample DG@Fe and a histogram shows the metal particle size distribution.

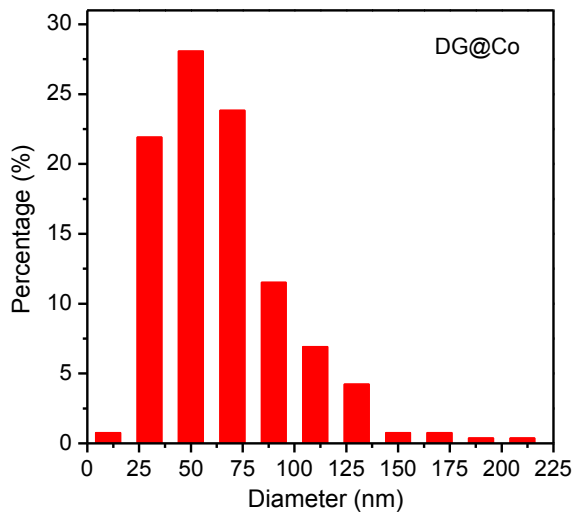
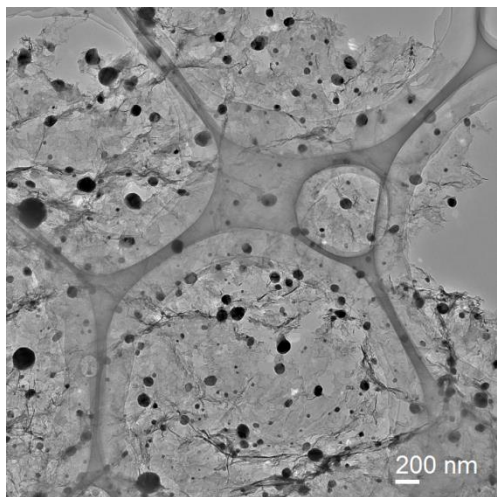


Fig. S6 TEM images of the prepared sample DG@Co and a histogram shows the metal particle size distribution.

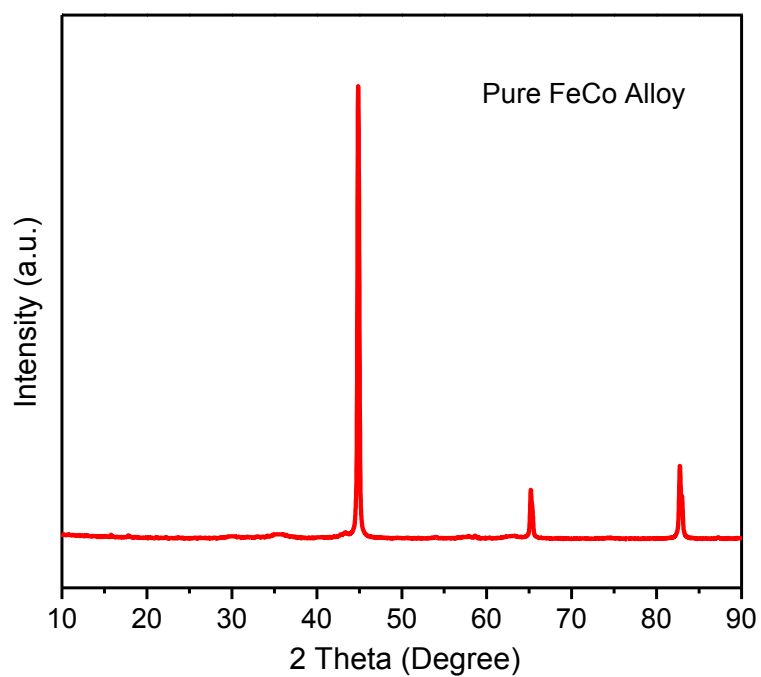


Fig. S7 XRD pattern of the synthesized sample FeCo.

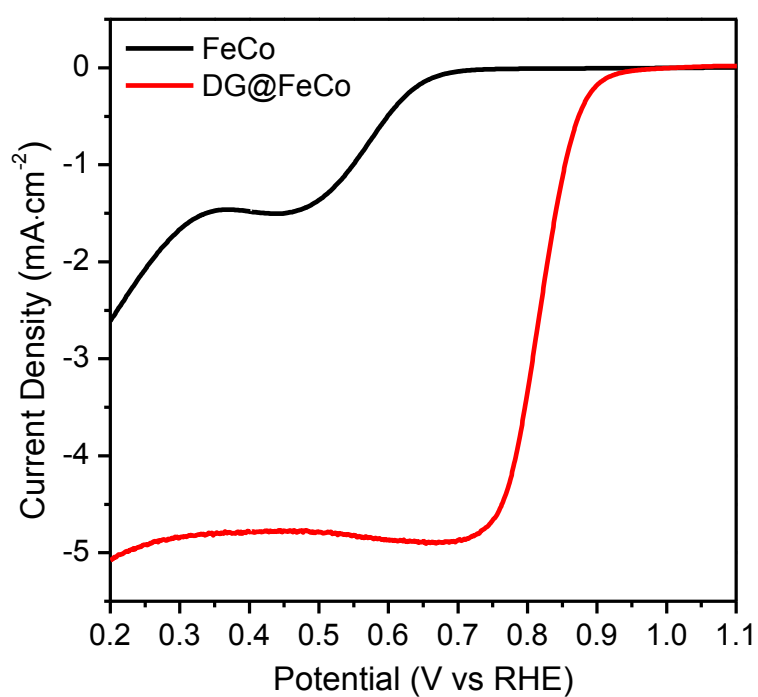


Fig. S8 LSV curves of the prepared samples pure FeCo alloy, and DG@FeCo measured at the rotation speed of 1600 rpm in an O₂-saturated 0.1 M KOH solution.

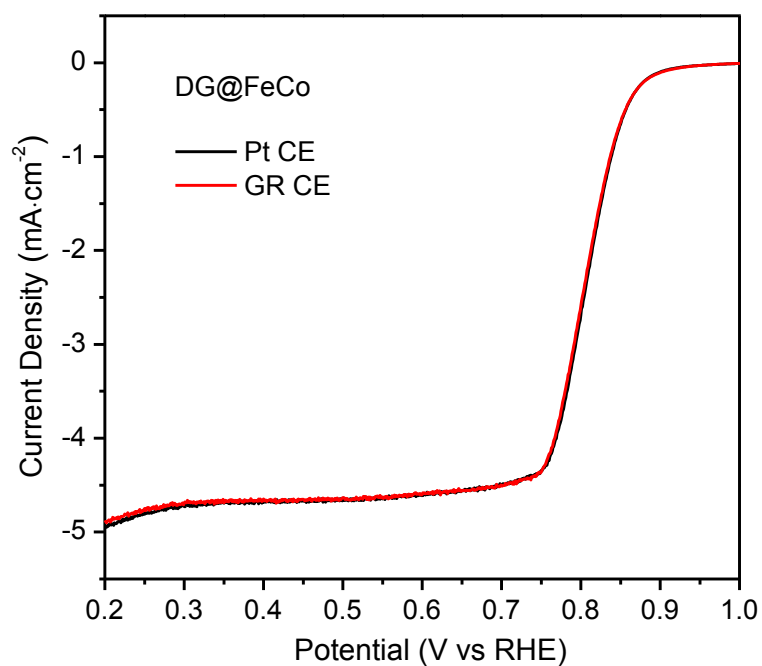


Fig. S9 ORR polarization curves of the sample DG@FeCo tested in an oxygen-saturated 0.1 M KOH solution using a Pt wire and a graphite rod as the counter electrode.

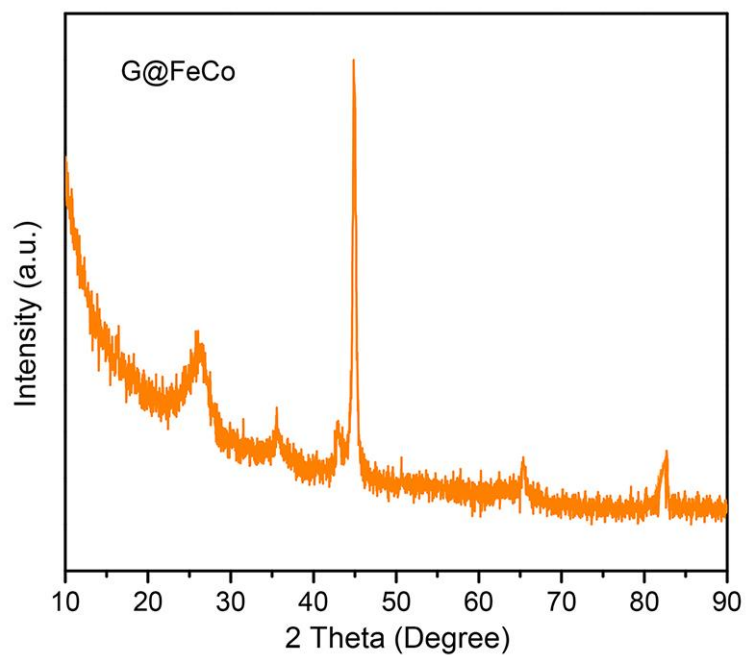


Fig. S10 XRD pattern of the synthesized sample G@FeCo.

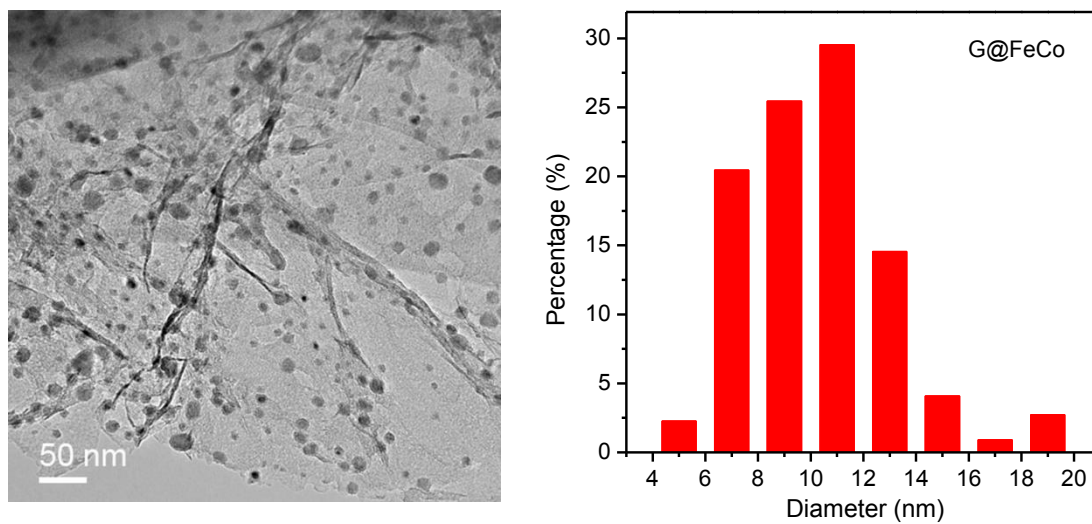


Fig. S11 TEM image of the synthesized sample G@FeCo a histogram shows the metal particle size distribution.

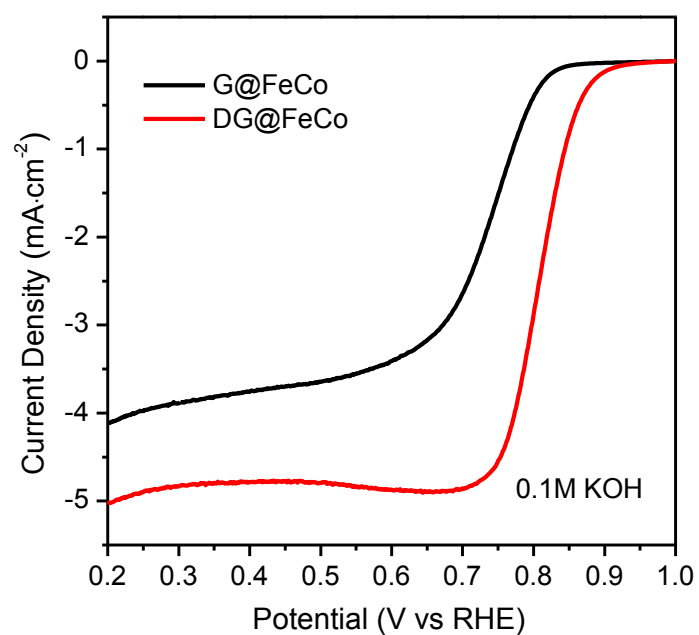


Fig. S12 LSV curves of the prepared samples G@FeCo, and DG@FeCo measured at the rotation speed of 1600 rpm in an O₂-saturated 0.1 M KOH solution.

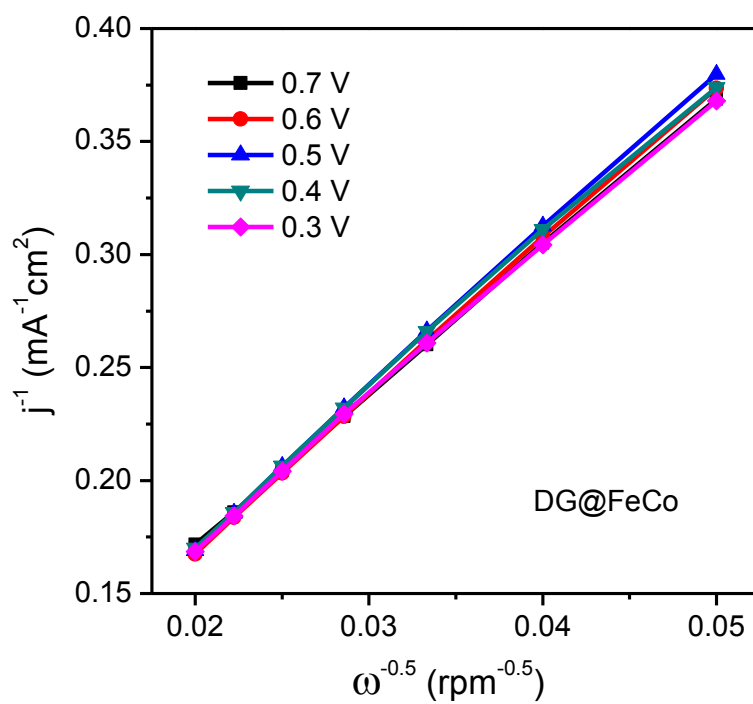


Fig. S13 K-L plots of the prepared sample DG@FeCo.

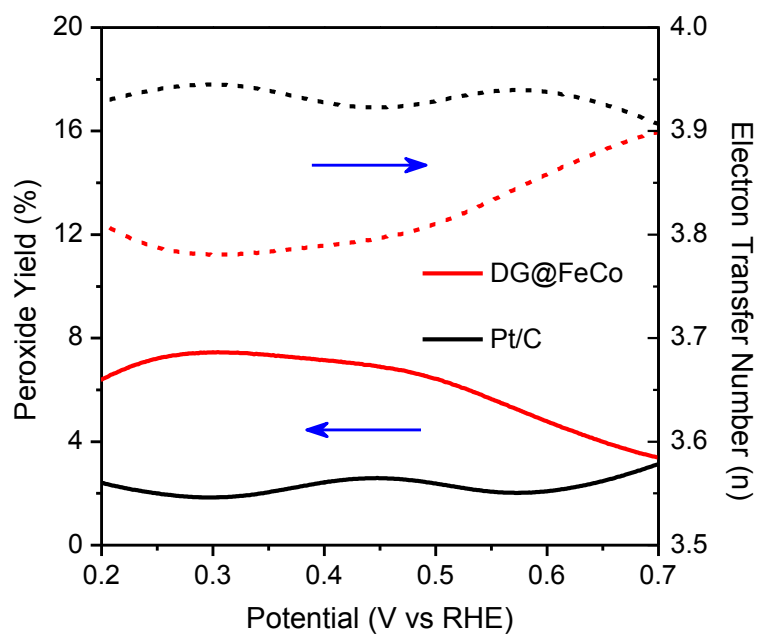


Fig. S14 Percentage of peroxide species (solid lines) and the electron transfer number (n) (dotted lines) of the DG@FeCo and the commercial Pt/C at different potentials.

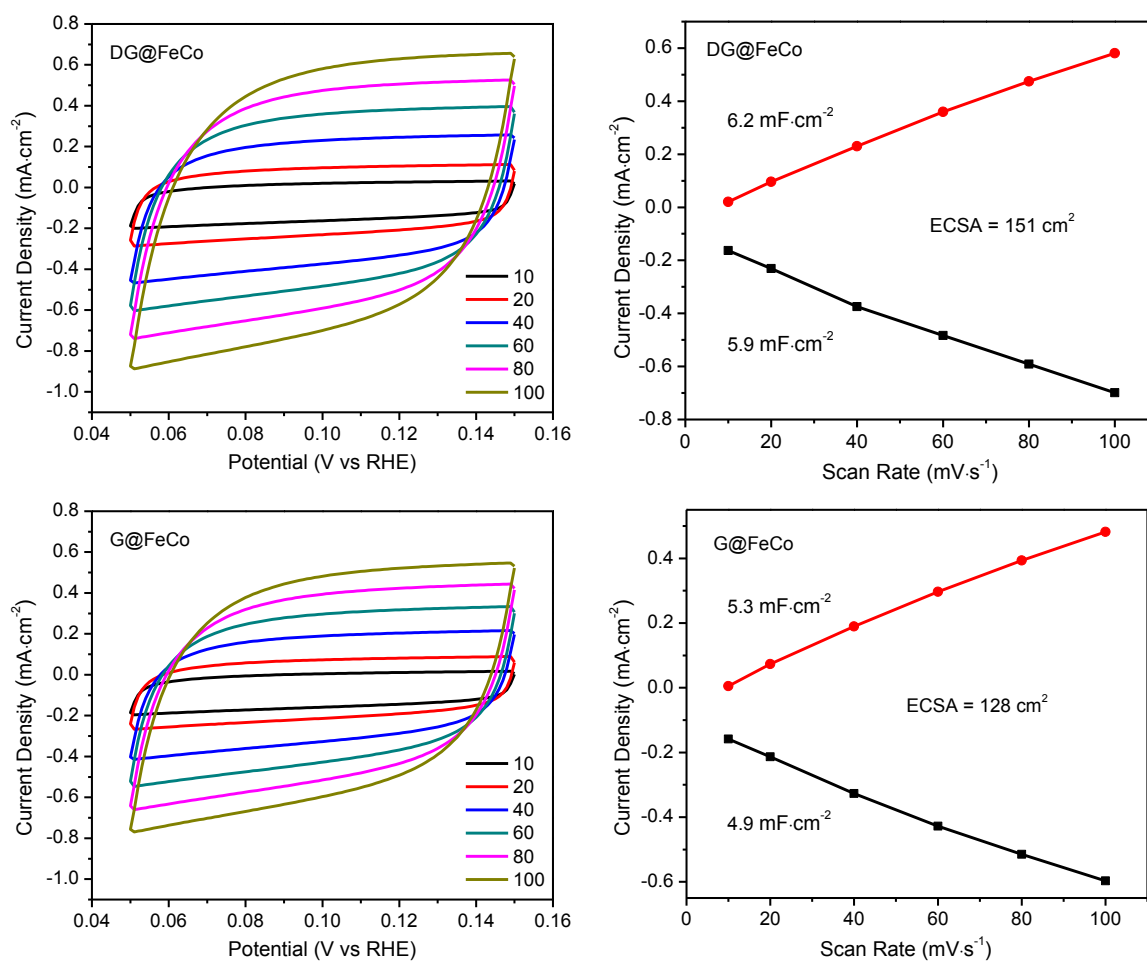


Fig. S15 Double-layer capacitance measurements for determining the electrochemical active surface area of the prepared samples DG@FeCo and G@FeCo.

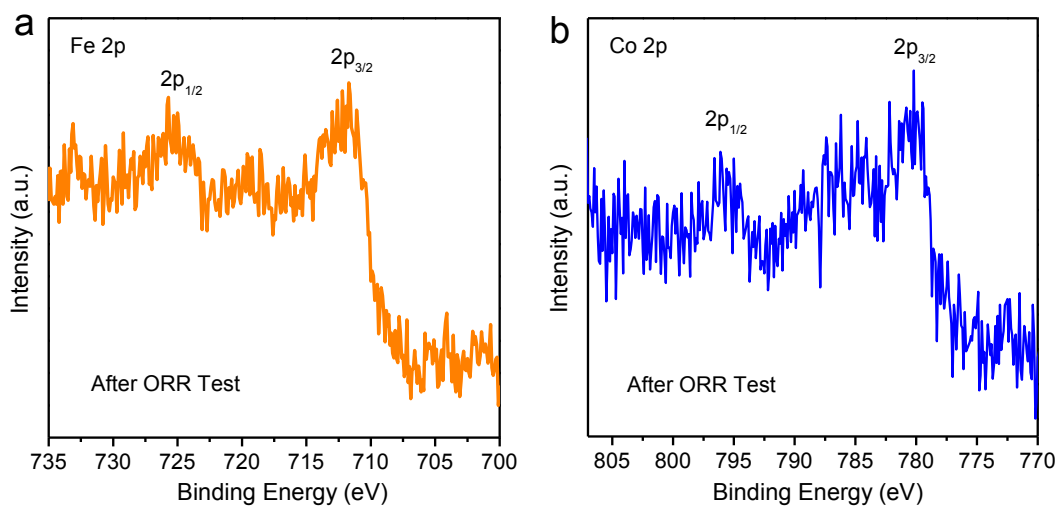


Fig. S16 (a) XPS high resolution Fe 2p XPS spectrum of DG@FeCo after the ORR test; (b) High resolution Co 2p XPS spectrum of DG@FeCo after the ORR test.

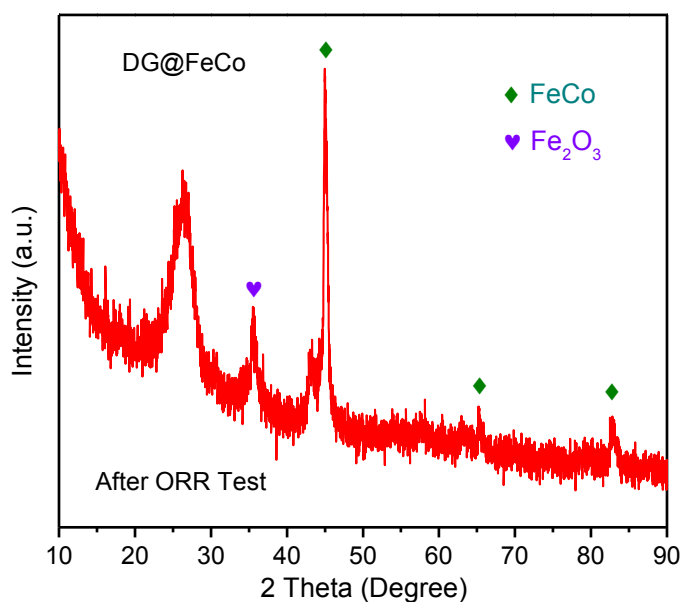


Fig. S17 XRD pattern of the DG@FeCo after the ORR test.

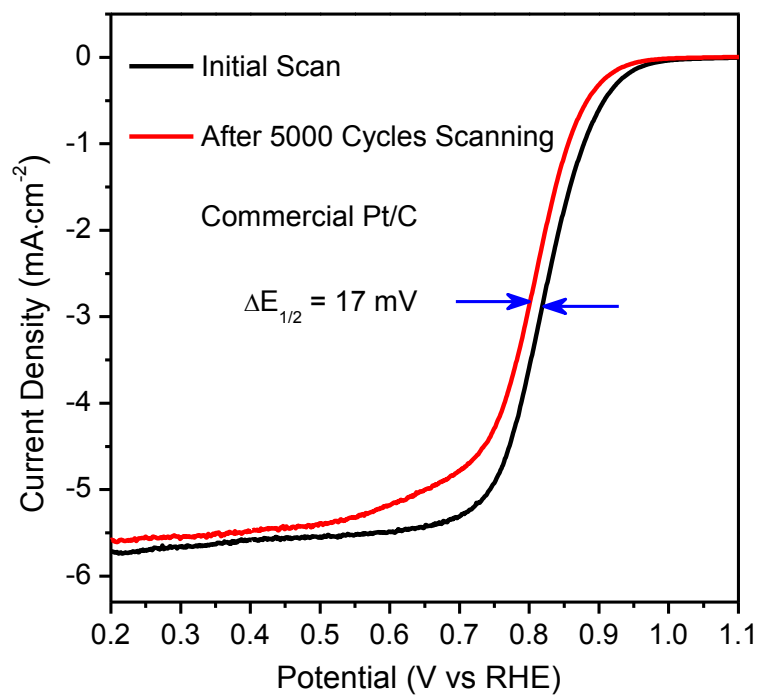


Fig. S18 Stability test results of the commercial Pt/C.

References

1. Y. Jia, L. Zhang, A. Du, G. Gao, J. Chen, X. Yan, C. L. Brown and X. Yao, *Adv. Mater.*, 2016, **28**, 9532-9538.
2. Y. Liang, H. Wang, J. Zhou, Y. Li, J. Wang, T. Regier and H. Dai, *J. Am. Chem. Soc.*, 2012, **134**, 3517-3523.
3. S. Wang, D. Yu, L. Dai, D. W. Chang and J.-B. Baek, *ACS Nano*, 2011, **5**, 6202-6209.
4. U. A. Paulus, T. J. Schmidt, H. A. Gasteiger and R. J. Behm, *J. Electroanal. Chem.*, 2001, **495**, 134-145.
5. Y. Liang, Y. Li, H. Wang, J. Zhou, J. Wang, T. Regier and H. Dai, *Nat. Mater.*, 2011, **10**, 780-786.